

See discussions, stats, and author profiles for this publication at: <https://www.researchgate.net/publication/45404903>

# Nucleation and Growth Kinetics of Electrodeposited Sulfate-Doped Polypyrrole: Determination of the Diffusion Coefficient of SO<sub>4</sub><sup>2-</sup> in the Polymeric Membrane

ARTICLE *in* THE JOURNAL OF PHYSICAL CHEMISTRY B · AUGUST 2010

Impact Factor: 3.3 · DOI: 10.1021/jp102676q · Source: PubMed

---

CITATIONS

19

READS

42

## 9 AUTHORS, INCLUDING:



Luis Humberto Mendoza-Huizar  
Autonomous University of Hidalgo

55 PUBLICATIONS 330 CITATIONS

[SEE PROFILE](#)



Manuel Palomar  
Metropolitan Autonomous University

112 PUBLICATIONS 1,595 CITATIONS

[SEE PROFILE](#)



Jorge Uruchurtu  
Universidad Autónoma del Estado de More...

188 PUBLICATIONS 622 CITATIONS

[SEE PROFILE](#)



Jose Manuel Juarez  
Centro Nacional de Metrologia

29 PUBLICATIONS 71 CITATIONS

[SEE PROFILE](#)

# Nucleation and Growth Kinetics of Electrodeposited Sulfate-Doped Polypyrrole: Determination of the Diffusion Coefficient of $\text{SO}_4^{2-}$ in the Polymeric Membrane

T. de J. Licona-Sánchez, G. A. Álvarez-Romero,\* L. H. Mendoza-Huizar, and C. A. Galán-Vidal

Área Académica de Química, Laboratorio de Química Analítica, Universidad Autónoma del Estado de Hidalgo, Ciudad Universitaria, Carretera Pachuca-Tulancingo Km. 4.5, Mineral de la Reforma, C.P. 42184, Hidalgo, México

M. Palomar-Pardavé,\* M. Romero-Romo, H. Herrera-Hernández, and J. Uruchurtu†

Departamento de Materiales, Universidad Autónoma Metropolitana-Azcapotzalco, Av. San Pablo 180, Col Reynosa Tamaulipas, C.P. 02200, México, D.F.

J. M. Juárez-García

Laboratorio de Microanálisis, Centro Nacional de Metrología, km 4.5 de la Carretera a los Cues, municipio de El Marqués, Querétaro, México

Received: March 24, 2010; Revised Manuscript Received: June 29, 2010

A kinetic study for the electrosynthesis of polypyrrole (Ppy) doped with  $\text{SO}_4^{2-}$  ions is presented. Ppy films were electrochemically polymerized onto a graphite-epoxy resin electrode. Experimental current density transients ( $j-t$ ) were obtained for three different potentiometric behaviors: anionic, cationic, and a combination. Theoretical models were used to fit the experimental  $j-t$  data to determine the nucleation and growth processes controlling the polymer synthesis. It was encountered that, in all cases, pyrrole electropolymerization involves two concomitant processes, namely, a Ppy diffusion limited multiple 3D nucleation and growth and pyrrole electro-oxidation on the growing surface of the Ppy nuclei. SEM analysis of the electrodes surfaces reveals that Ppy deposition occurred over most of the electrode surface by multiple nucleation of hemispheres, as the theoretical model used for the analysis of the current transients required. Hemispherical particles formed the polymeric film displaying different sizes. The order for the particle size was as follows: anionic > anionic–cationic > cationic. These results are congruent with those obtained by theoretical analysis of the corresponding current transients. Analysis of the impedance measurements recorded on the anionic Ppy film, immersed in an aqueous solution with different sulfate ion concentrations evidenced that  $\text{SO}_4^{2-}$  ions diffuse through the Ppy film provoking a decrease of its electrical resistance and an increase of its dielectric constant. From the Warburg impedance coefficient, the sulfate coefficient of diffusion in the Ppy film was  $1.38 \times 10^{-9} \text{ cm}^2 \text{ s}^{-1}$ .

## 1. Introduction

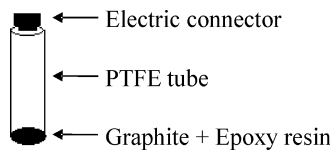
The analysis of experimental current density transients, recorded during electrochemical phase formation processes,<sup>1,2</sup> provides valuable information regarding the kinetics of this type of electrochemical processes such as nucleation kinetics, dimensional growth, superposition of growth centers, and morphology. The knowledge of the electrosynthesis kinetics helps to characterize the variables involved in the process, which will have direct influence on the final properties and characteristics of the so formed material.<sup>3</sup> In this case, the formation of a new phase is induced by an electrical potential perturbation, starting with a nucleation stage, that strongly depends on the different electrosynthesis conditions and the overpotential imposed.<sup>4–7</sup> The potentiostatic current density transients corresponding to these systems show a typical current increase with

time, which is related to the nucleation and growth processes of the new phase over the electrode surface.<sup>4,8</sup> Some examples of electrochemical processes that involve a phase formation are the following: metal electrodeposition,<sup>9</sup> anodic film formation,<sup>10</sup> micelles adsorption,<sup>11</sup> and the electrochemical synthesis of conducting polymers.<sup>12–15</sup> Theoretical models have been proposed to explain the electrochemical behavior of conducting polymers,<sup>16</sup> that determine the kinetics for the formation and growth of nuclei, and also the growth type (dimension); such models describe also the rate law for the formation of nuclei on a finite number of active sites, which are distributed randomly over the electrode surface,<sup>17</sup> taking into account the nature and superficial texture of the substrate,<sup>18–20</sup> the limiting stage of the overall process, nuclei geometry, the possible formation of a superficial layer because of ionization or anodic oxidation of the electrode's surface, and the electrochemical synthesis procedure.<sup>21,22</sup> The shape of the growing centers determines, in many cases, the shape of the corresponding current density transient for a specific potential.<sup>23</sup> If nuclei growth is confined to an  $x-y$  plane over the electrode's surface, the nucleation and growth processes are said to happen in two dimensions

\* To whom correspondence should be addressed. E-mail: gian@uaeh.edu.mx and mepp@correo.azc.uam.mx.

† On sabbatical leave. Permanent address: Centro de Investigación en Ingeniería y Ciencias Aplicadas, Universidad Autónoma del Estado de Morelos, Av. Universidad 1001, Col. Chamilpa, Cuernavaca, Mor.

**SCHEME 1:** Representation of the Graphite–Epoxy Resin Composite Used As Working Electrodes for the Electrochemical Synthesis of Ppy- $\text{SO}_4^{2-}$  Films



(2D).<sup>24–26</sup> When nuclei grow as hemispheres or cones, the nucleation and growth process happens in three dimensions (3D).<sup>22,24,27–30</sup> Due to the increasing number of practical applications<sup>31–38</sup> of conducting polymers, like polypyrrole (Ppy),<sup>37,38</sup> experimental and theoretical reports also have increased during the last years, especially those studying the relations between the potentiostatic parameters used for the electropolymerization and the resulting morphology and properties. However, there are few reports about kinetic parameters for the conducting polymers electrosynthesis occurring in the presence of doping agents. Sulfate ion as polypyrrole dopant displays very peculiar characteristics that significantly differ from those of other ions commonly used to dope the polymer,<sup>37,38</sup> which implies a significant number of possible applications for this kind of polymers,<sup>31,39</sup> like the development of highly selective chemical sensors,<sup>40,41</sup> application as artificial muscles,<sup>12,42–44</sup> anticorrosive coatings,<sup>45–48</sup> etc.

In this work the kinetics of electrochemically synthesized sulfate-doped polypyrrole films, Ppy- $\text{SO}_4^{2-}$ , with different potentiometric response, namely those whose potential varies with the presence of anions (anionic polypyrrole), with cations (cationic polypyrrole), or both (anionic–cationic polypyrrole),<sup>49</sup> is studied.

## 2. Experimental Section

**2.1. Reagents.** All reagents used in this work were analytical grade.  $\text{Na}_2\text{SO}_4$  (Aldrich) was used as supporting electrolyte and source of sulfate ions. Pyrrole (Py) (Aldrich) was purified by distillation with  $\text{N}_2$  atmosphere. Ultrapure monocrystalline graphite powder 99,999% and Araldit epoxy resin with H.Y hardener were used to construct the working electrode. All solutions were prepared with deionized water obtained from a Milli Q (Millipore) system with 18.2  $\text{M}\Omega \text{ cm}$  resistivity. The solutions of Py containing  $\text{SO}_4^{2-}$  were bubbled with pure  $\text{N}_2$  before each experiment.

**2.2. Instrumentation.** A typical three-electrode cell was used: a platinum wire was used as counter electrode, an Ag/AgCl (900200 Orion) as reference electrode, and carbon–epoxy composite as working electrode. The composite electrode was prepared by mixing graphite powder and Araldit epoxy resin–H.Y hardener (agglomerating agent in a 1:0.4 proportion) components in a 60:40 proportion relation. The proportion of the composite was supported by using a 0.5 cm diameter PTFE tube with an electrical contact, as shown in Scheme 1. The hardening of the composite was achieved during a period of 12 h at a constant temperature of 60 °C. Thereafter, the exposed surface was polished before the electrochemical growth of the polypyrrole film. Polypyrrole (Ppy) films were obtained potentiostatically and potentiodynamically by using an electrochemical workstation (Ecochemie) PGSTAT 30 AUTOLAB. For the electrochemical impedance, EIS, measurements a BAS-Zahner IM6 electrochemical workstation was used. OriginLab version 6.1 software was used for the fitting analysis.

**2.3. Electrochemical Synthesis of Ppy- $\text{SO}_4^{2-}$  Films.** Ppy- $\text{SO}_4^{2-}$  films were synthesized by cyclic voltammetry and chronamperometric techniques over the exposed surface of the

**TABLE 1: Experimental Conditions Required to Produce Ppy- $\text{SO}_4^{2-}$  Films with Different Potentiometric Responses**

synthesis parameter	potentiometric response		
	anionic	cationic	anionic–cationic
E/V	0.86–0.96	0.80–1.00	0.52–0.86
t/min	10.8–15.0	6.0–10.0	4.00–15.0
[Py]/mol L <sup>-1</sup>	0.28–0.40	0.05–0.4	0.05–0.225
[ $\text{SO}_4^{2-}$ ]/mol L <sup>-1</sup>	0.35–0.54	0.005–0.5	0.005–0.35

composite electrode. In our previous research<sup>49</sup> we have found that depending on the potentiostatic conditions imposed, different potentiometric responses can be achieved for the Ppy- $\text{SO}_4^{2-}$  film, namely, anionic, cationic, or anionic–cationic combination; therefore these polymeric films can be used to produce different kinds of electrochemical sensors.<sup>12,13,37</sup> On the basis of these results, we have already suggested the limiting values for the electrochemical synthesis parameters; these are shown in Table 1.

These results were used to synthesize a series of Ppy- $\text{SO}_4^{2-}$  films with the three different behaviors.

**2.4. SEM Characterization.** Subsequent to the electrochemical synthesis of the Ppy- $\text{SO}_4^{2-}$  films, the samples were examined by means of an Electron Probe Microanalyzer (EPMA) with 3 WDS/EDS combined JXA-8200 (JEOL), using an accelerating voltage of 15 kV.

## 3. Results and Discussion

**3.1. Potentiodynamic Synthesis.** Figure 1 shows a typical cyclic voltammogram obtained during potentiodynamic synthesis of a Ppy- $\text{SO}_4^{2-}$  film: the potential scan started at the null-current potential and cycles programmed in an interval from –1200 to 1200 mV in the anodic direction with a scan rate of 100 mV s<sup>-1</sup>. The oxidation charge density,  $Q$ , obtained (Figure 1 inset) reaches a maximum value at about 50 cycles. This behavior is typical for the electrochemical formation of conducting polymers<sup>12,13</sup> and indicates that the amount of polymer on the electrode surface increases as the number of cycles increases.

**3.2. Potentiostatic Synthesis.** Figure 2 shows families of current–density transients for each of the potentiometric responses encountered. The similarity in the shape of the transients suggests that the nucleation and growth mechanisms involved in all cases are the same. However, it is clear that the charge involved (the area under the  $j$ – $t$  plots) in each case is quite different.

Recently, Palomar-Pardavé et al.<sup>9</sup> have proposed a theoretical physicochemical model that describes  $j$ – $t$  plots with a very similar shape to those shown in Figure 2. It is relevant to stress that this model is not merely a mathematical description of the experimental current transients, because each parameter involved (see eqs 3–6) has a clear physical meaning. According to them,<sup>9</sup> this sort of  $j$ – $t$  plot is obtained when the potentiostatic formation of a new phase, on the electrode surface, involves the presence of two simultaneous electrode reactions, namely, a multiple hemispherical 3D nucleation and growth limited by the mass transfer reaction,  $J_{3D}(t)$ , presently, Ppy, nucleation and growth as well as another faradaic process occurring on the growing surfaces of the new phase, in this case pyrrole oxidation on the Ppy surface,  $J_{PO}(t)$ . Thus, in our case, the equation derived describing this process is:

$$J_{\text{total}}(t) = J_{3D}(t) + J_{PO}(t) \quad (1)$$

where the overall current density–time transient,  $J_{\text{total}}(t)$ , is given by the addition of the contributions due to pyrrole oxidation on

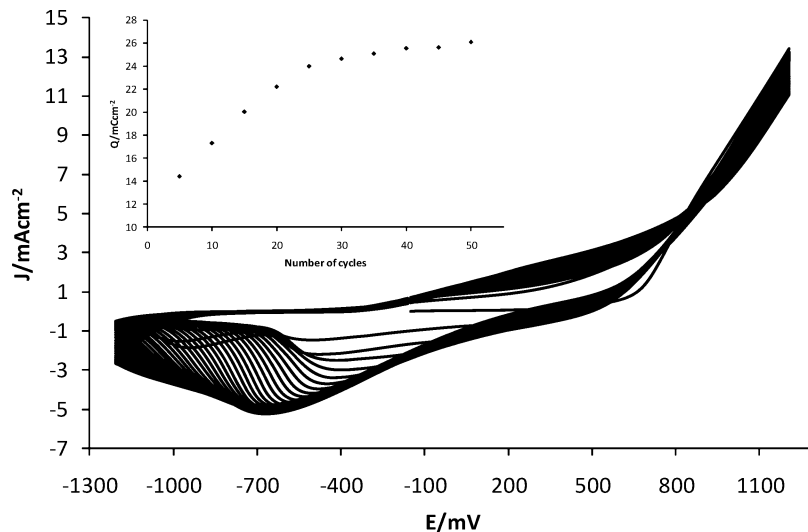


**Figure 1.** Cyclic voltammograms for the potentiodynamic synthesis of Ppy-SO<sub>4</sub><sup>2-</sup> using a composite electrode, [Py] = 0.1 M, [SO<sub>4</sub><sup>2-</sup>] = 0.1 M, 50 cycles, and a scan rate of 100 mV s<sup>-1</sup>. The inset shows the variation of the oxidation charge density recorded from integration of the anodic branches of the voltammograms.

the bare electrode surface, oligomer formation, and subsequently after nucleation and growth of the polypyrrole deposit,  $J_{3D}(t)$ , and that due to the pyrrole oxidation,  $J_{PO}(t)$ , on the growing polypyrrole surface. Furthermore, this contribution to the overall current density transient may also take into account that due to polypyrrole oxidation, which is believed to occur at a much lower potential than monomer oxidation thus occurring immediately after the polymer is formed. Notwithstanding, even when the polymer could be considered to have pores, which may allow monomer diffusion and oxidation on the electrode surface, in our model this contribution is considered negligible when compared with monomer oxidation on the growing polypyrrole surface.

Equation 1 can be parametrized as follows (see ref 9):

$$J_{\text{total}}(t) = (P_1 + P_4 t^{-1/2}) \left( 1 - \exp \left\{ -P_2 \left[ t - \frac{1 - \exp(-P_3 t)}{P_3} \right] \right\} \right) \quad (2)$$

with

$$P_1 = \left( \frac{2c_0 M}{\pi \rho} \right)^{1/2} z_{PO} F k_{PO} \quad (3)$$

$$P_2 = N_0 \pi k' D \quad (4)$$

$$P_3 = A \quad (5)$$

$$P_4 = \frac{zFD^{1/2}c_0}{\pi^{1/2}} \quad (6)$$

$$k' = (8\pi c_0 / \rho)^{1/2} \quad (7)$$

where  $c_0$  is the pyrrole bulk solution concentration,  $F$  is the Faraday constant,  $\rho$  is the density of the deposit,  $M$  is its molar mass,  $z_{PO}F$  is the molar charge transferred during the pyrrole

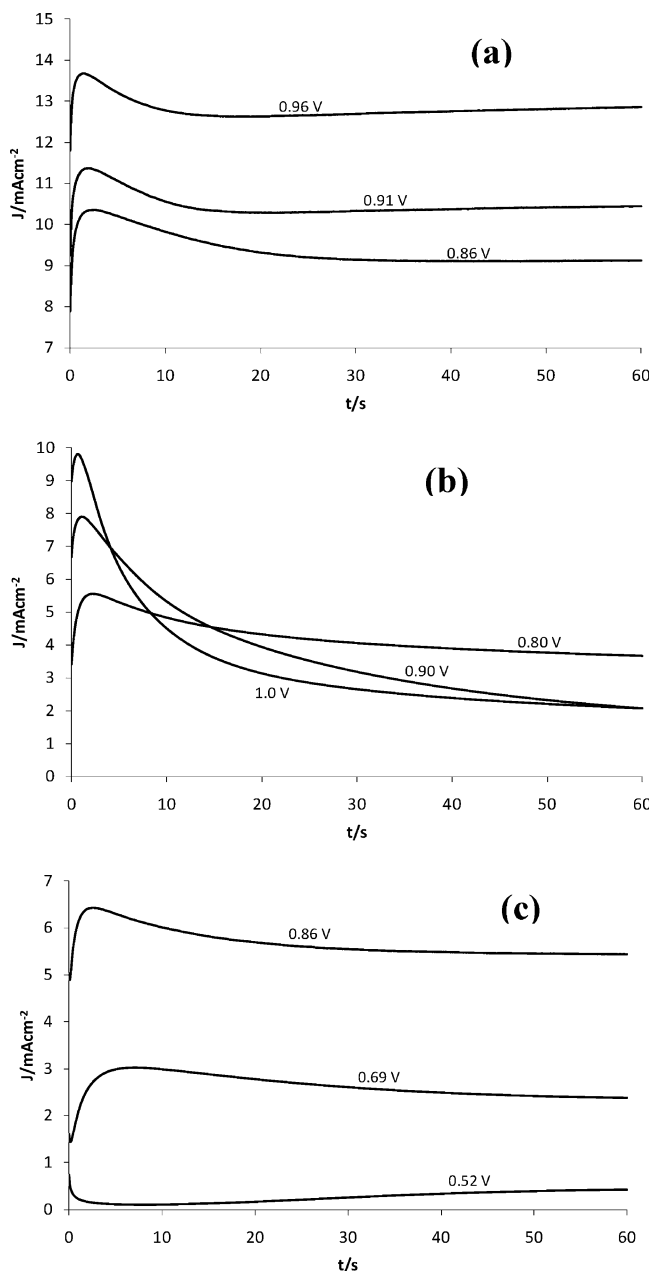
oxidation process,  $k_{PO}$  is the rate constant for pyrrole oxidation reaction on the polypyrrole surface,  $D$  is the pyrrole diffusion coefficient,  $A$  is the polypyrrole nucleation rate, and  $N_0$  is the number density of active sites for polypyrrole nucleation on the electrode surface.

Figure 3 shows a comparison of the experimental  $j-t$  plot recorded during polypyrrole nucleation and growth, see Figure 2, and the theoretical current density transient generated by nonlinear fit of eq 2 to the experimental data.

The theoretical model represented by eq 1 describes adequately the whole current density transient recorded in all cases. From this analysis, the kinetics parameters  $A$  and  $N_0$  were obtained, see Table 2, from which it is clear that the potentiostatic response of the Ppy-SO<sub>4</sub><sup>2-</sup> film does not change the nucleation rate; however, the number density of active sites is affected. It is important to mention that  $k_{PO}$  could be estimated from  $P_1$  value, see eq 3, knowing the polypyrrole density, 1.5 g cm<sup>-3</sup>, which is a physical constant, reported in the literature.<sup>50</sup> However, in this work an estimate of  $k_{PO}$  is not included due to the difficulty in finding a reliable value for polypyrrole molar mass.

From Figure 3 it is also possible to note that part of the current measured during this sort of transients is effectively used for the polymer growth on the electrode surface, related with  $J_{3D}$ , and the rest,  $J_{PO}$ , is used for Py oxidation on the Ppy surface, which helps for the subsequent Ppy growth. In this respect one can infer by comparison of the transients presented in Figure 3 that the Ppy-SO<sub>4</sub><sup>2-</sup> film with a potential sensible to anions involves a larger amount of deposited polymer. Moreover, that the anionic-cationic response is in turn greater than that associated with the cationic response.

**3.2.1. SEM Characterization.** Figure 4 shows the morphology characteristics of the bare graphite-epoxy resin electrode surface, see Figure 4a, and those coated with the Ppy-SO<sub>4</sub><sup>2-</sup> films that display different potentiometric responses namely cationic, Figure 4b, anionic-cationic, Figure 4c, and anionic, Figure 4d. From these images one could clearly note that Ppy deposition actually occurred over most of the electrode surface by multiple nucleation of hemispheres, as the theoretical model used for the analysis of the current transients required. In all cases the hemispherical particles that form the polymeric film



**Figure 2.** Typical current–density transients recorded during the electrochemical synthesis of Ppy- $\text{SO}_4^{2-}$  films, with different potentiometric response, on the graphite–epoxy resin composite: (a) anionic [ $\text{SO}_4^{2-}$ ] = 0.5 M, [Py] = 0.3 M, time ( $t$ ) = 774 s; (b) cationic [ $\text{SO}_4^{2-}$ ] = 0.5 M, [Py] = 0.05 M,  $t$  = 480 s; (c) anionic–cationic [ $\text{SO}_4^{2-}$ ] = 0.17 M, [Py] = 0.13 M,  $t$  = 570 s. The applied potentials used for the synthesis are indicated in the figure.

display different sizes depending on the electrochemical synthesis parameters. The order for the particle size is as follows: anionic > anionic–cationic > cationic. These results are consistent with those obtained by theoretical analysis of the corresponding current transients, see Table 2.

Figure 5 depicts the potentiometric response of the graphite–epoxy resin composite electrode modified with the potentiostatically formed anionic film in the presence of varying concentration of sulfate ions in solution; a log relationship was clearly obtained.

**3.2.2. EIS Evaluation of the Electrode Coated with the Ppy- $\text{SO}_4^{2-}$  Film That Displays a Potentiometric Anionic Response.** To evaluate the electrochemical properties of the anionic Ppy- $\text{SO}_4^{2-}$  film, electrochemical impedance measure-

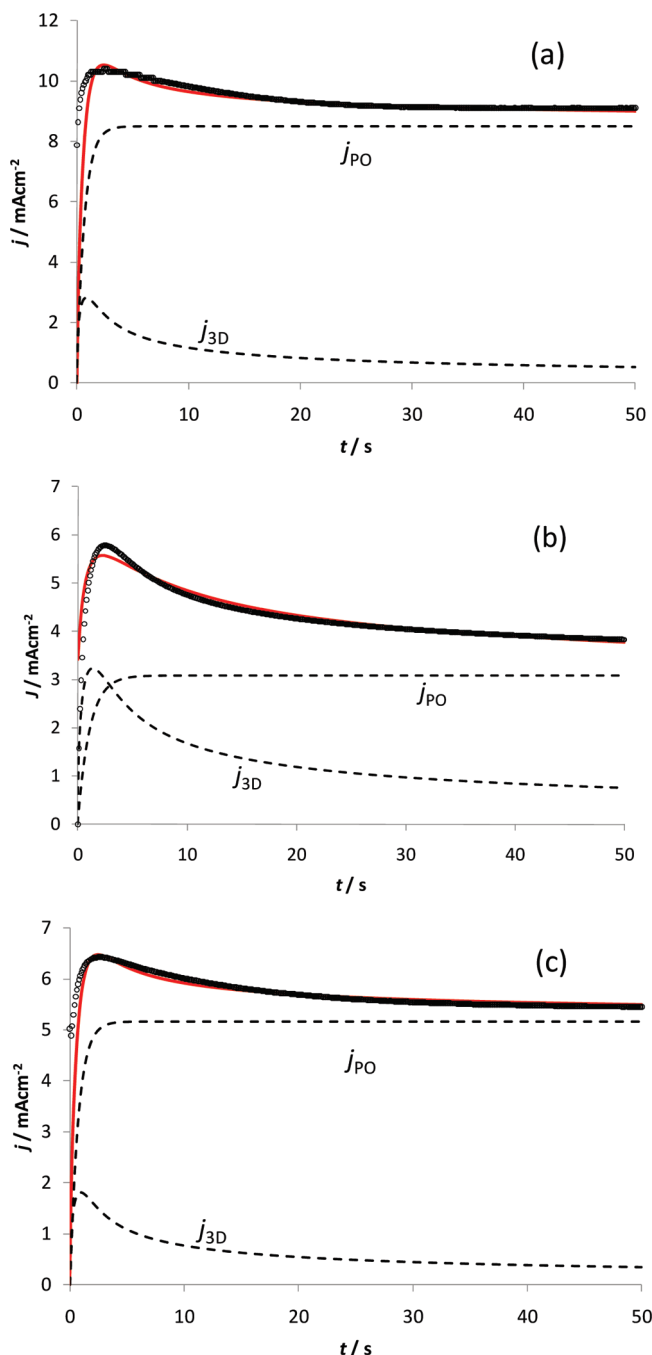


**Figure 3.** Comparison between an experimental current–density transient (---) recorded for each of the potentiostatic response (a) anionic response, (b) cationic response, and (c) anionic–cationic response, see Figure 2, and the theoretical current density transient (—) generated by the nonlinear fitting of eq 2 to the experimental data. Individual contributions due to  $J_{\text{PO}}$  and  $J_{\text{3D}}$  are also shown.

**TABLE 2: Kinetic Parameters Obtained after the Statistical Fit for the Three Different Potentiometric Responses**

type of response of the polymeric membrane	$10^{-4} N_0 / \text{cm}^{-2}$	$A / \text{s}^{-1}$
anionic	415	100
anionic–cationic	175	100
cationic	8.6	100

ments were recorded in the graphite–epoxy resin composite electrode, coated with the anionic Ppy- $\text{SO}_4^{2-}$  film, immersed

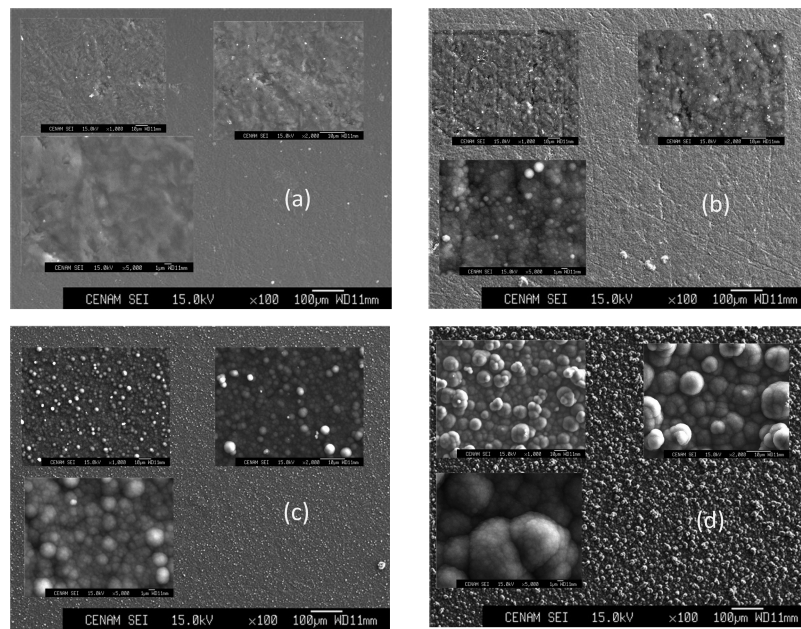


**Figure 4.** Secondary electron images,  $\times 100$ , of the bare graphite–epoxy resin electrode surface (a) and those coated with the  $\text{Ppy}-\text{SO}_4^{2-}$  films with different potentiometric responses: cationic (b), anionic–cationic (c), and anionic (d). The insets show, in each case, three different magnifications ( $\times 1000$ ,  $\times 2000$ , and  $\times 5000$ ).

in an aqueous solution with different  $\text{Na}_2\text{SO}_4$  concentrations. Figure 6 shows both the Nyquist and Bode impedance plots recorded.

On the basis of the shape of the Nyquist and Bode plots it was decided to use the equivalent circuit presented in Figure 7 to fit into the impedance measurements. This is a mathematical fitting of basic functions related to the classical electrical components (resistors, capacitors, inductors) plus a few specialized electrochemical elements (such as Warburg diffusion elements), see Table 3. In this circuit constant phase elements (CPE) were considered, rather than pure capacitors, in order to take into account the electrode surface roughness.<sup>51</sup>

Mathematically, a CPE's admittance is given by

$$1/Z = Y = Q^0(j\omega)^n \quad (8)$$

where  $Q^0$  has the numerical value of the admittance. When  $n = 1$ , this is the same equation as that for the impedance of a capacitor, where  $Q^0 = C$ .

$$1/Z = Y = j\omega Q^0 = j\omega C \quad (9)$$

When  $n$  is close to 1, the CPE resembles a capacitor, the phase angle not being  $90^\circ$ , but it is constant and somewhat less than  $90^\circ$  at all frequencies. In some cases, the *true* capacitance ( $C$ ) can be calculated from  $Q^0$  and  $n$ .

For the case of a CPE in parallel with a resistance, Hsu and Mansfeld<sup>52</sup> proposed eq 10 for calculating the *true* capacitance,  $C$ , as:

$$C = Q^0(\omega_{\text{MAX}})^{n-1} \quad (10)$$

In this equation,  $\omega_{\text{MAX}}$  represents the frequency at which the imaginary component reaches a maximum. It is the frequency at the top of the depressed semicircle, and it is also the frequency

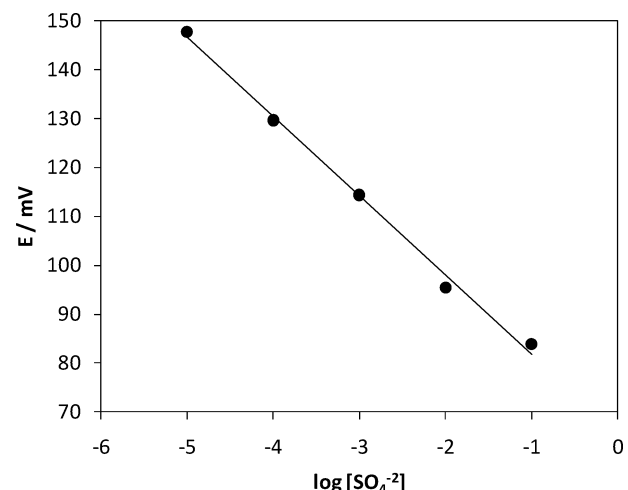


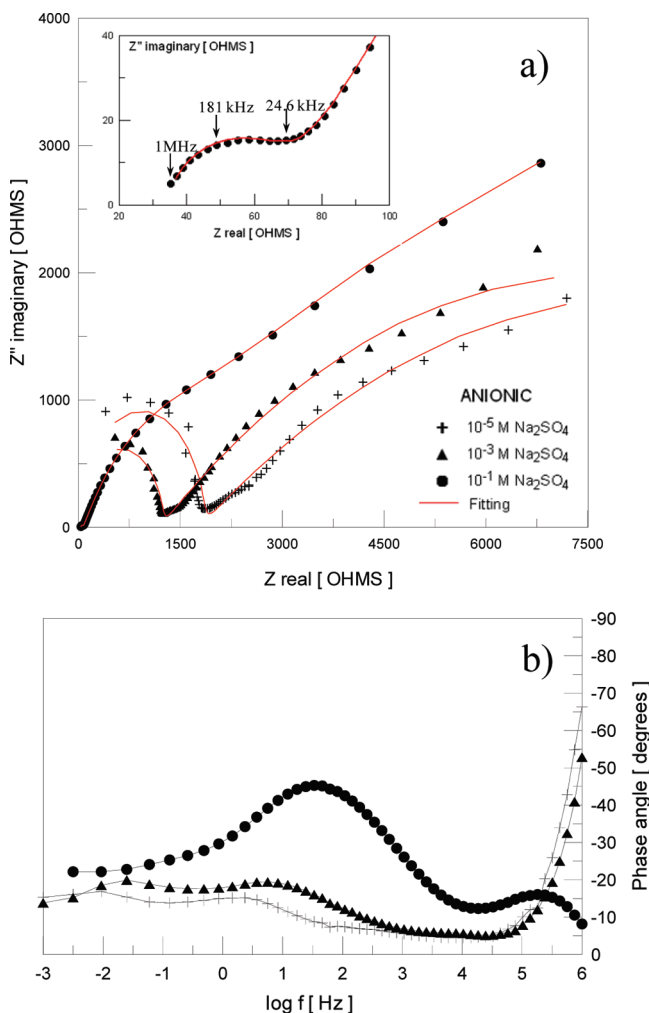
**Figure 5.** Electrode potential variation (●) of the graphite–epoxy resin composite electrode modified with the potentiostatically formed anionic film as a function of sulfate ions concentration. The line represents the linear fitting of the experimental points.

at which the real part ( $Z_{\text{real}}$ ) is midway between the low and high frequency  $x$ -axis intercepts.

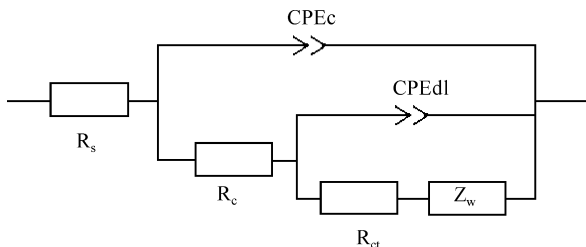
The equivalent circuit in Figure 6 includes the solution resistance ( $R_s$ ), a CPE associated to the polymer film (CPE<sub>c</sub>), the polymer resistance ( $R_c$ ), a CPE associated to the double layer interface (CPE<sub>dl</sub>), the charge transfer or polarization resistance ( $R_p$ ), and the Warburg impedance of the polymer ( $Z_w$ ).

Figure 6 compares the experimental impedance measurements (see Figure 6a) with those obtained by nonlinear fitting of the experimental data with the equivalent circuit shown in Figure 7. The best fitting parameters obtained are shown in Table 3.

From Table 3, it becomes clear that  $\text{Ppy}-\text{SO}_4^{2-}$  film resistance  $R_c$  values decreased and its capacitance values  $C_c$  increased with the increase of sulfate ion concentrations. Since the geometry of the polymeric film, namely, the surface area  $A$  and thickness  $\delta$ , were the same in all cases; the observed increase in the



**Figure 6.** Nyquist (a) and Bode (b) impedance plots recorded for the graphite–epoxy resin composite electrode, coated with the Ppy– $\text{SO}_4^{2-}$  film, immersed in an aqueous solution with different  $\text{Na}_2\text{SO}_4$  concentrations as indicated in the figure. The solid lines in the Nyquist plots were obtained by nonlinear fitting of the experimental data with the equivalent circuit shown in Figure 7. The inset in panel a depicts a close-up of a higher frequency semicircle.



**Figure 7.** Proposed electrical equivalent circuit used to simulate the experimental impedance plots.

capacitance should be associated to an increment in the local dielectric constant; as can be noted from the well-known Helmholtz model:

$$C_c = \frac{\epsilon_c \epsilon_0 A}{\delta} \quad (11)$$

where  $\omega_c$  is the dielectric constant of the polymer,  $\epsilon_0$  is the vacuum permittivity,  $A$  is the electrode surface area, and  $\delta$  is the thickness of the protective layer. The previous observation

**TABLE 3: Impedance Parameters of the Graphite-Epoxy Resin Electrode Coated with the Ppy– $\text{SO}_4^{2-}$  Film, that Display a Potentiostatic Anionic Response, Immersed in an Aqueous Solution Containing Different  $[\text{Na}_2\text{SO}_4]$ , Using the Equivalent Circuit Shown in Figure 7**

$[\text{Na}_2\text{SO}_4]/\text{M}$	$10^{10}C_c^a/\text{F cm}^{-2}$	$R_c^a/\Omega \text{cm}^2$	$n$	$10^4C_{dl}^a/\text{F cm}^{-2}$	$R_{ct}/\text{K}\Omega \text{cm}^2$	$n$	$Z_w/\Omega \text{cm}^2 \text{s}^{-1/2}$
$10^{-5}$	4.98	510	1	8.6	3.74	0.3	
$10^{-3}$	5.13	340	1	4.2	4.01	0.3	
$10^{-1}$	11820	106	0.8	2.7	4.1	0.8	257.5

<sup>a</sup> Both the capacitance of the polymeric film ( $C_c$ ) and the double layer capacitance ( $C_{dl}$ ) were obtained from the values of CPEc and CPEdl, respectively, using eq 10.

regarding variations of  $R_c$  and  $C_c$  with sulfate ions in solution strongly suggests that the  $\text{SO}_4^{2-}$  ions in solution can penetrate the polymeric film. Moreover, the diffusion coefficient for the ionic transport in the polymeric matrix can be obtained with the impedance measurements by using the Warburg impedance coefficient  $Z_w$ , from eq 12:<sup>53</sup>

$$D = \left[ \frac{RT}{\sqrt{2}AF^2Z_wC} \right]^2 \quad (12)$$

where  $D$  is the diffusion coefficient of sulfate ions ( $\text{cm}^2 \text{s}^{-1}$ ),  $A$  is the area of electrode ( $\text{cm}^2$ ),  $Z_w$  is the Warburg impedance coefficient ( $\Omega \text{cm}^2 \text{s}^{-1/2}$ ),  $C$  is the concentration of sulfate (mol  $\text{cm}^{-3}$ ),  $R$  is the gas constant ( $\text{J K}^{-1} \text{mol}^{-1}$ ),  $T$  is the absolute temperature (K), and  $F$  is the Faraday constant ( $\text{C mol}^{-1}$ ). The result of the calculation is  $1.38 \times 10^{-9} \text{ cm}^2 \text{s}^{-1}$ . It is important to stress that Otero et al.,<sup>54,55</sup> using chronoamperometry, reported similar values for the perchlorate diffusion coefficient in swelling polypyrrole ( $0.4 \times 10^{-9}$  to  $2.2 \times 10^{-9} \text{ cm}^2 \text{s}^{-1}$ )<sup>54</sup> and in polypyrrole with different degrees of degradation (by overoxidation) ( $0.4 \times 10^{-9}$  to  $1.8 \times 10^{-9} \text{ cm}^2 \text{s}^{-1}$ ).<sup>55</sup> Moreover, Kępas and Grzeszczuk,<sup>56</sup> using EIS measurements, determined the diffusion coefficients for hexafluorosilicate and hexafluoroaluminate counterion systems in the order of  $10^{-10} \text{ cm}^2 \text{s}^{-1}$ .

#### 4. Conclusions

From the potentiostatic step technique and EIS it was shown that sulfate-doped pyrrole electropolymerization involved two concomitant processes, namely, a Ppy diffusion limited multiple 3D nucleation and growth and pyrrole electro-oxidation on the growing surface of the Ppy nuclei. From SEM analysis it was shown that Ppy deposition occurred over most of the electrode surface by multiple nucleation of hemispheres, as the theoretical model used for the analysis of the current transients required. The order for the particle size was as follows: anionic > anionic–cationic > cationic. These results are congruent with those obtained by theoretical analysis of the corresponding current transients. Analysis of the impedance measurements recorded on the anionic Ppy film, immersed in an aqueous solution with different sulfate ion concentrations evidenced that  $\text{SO}_4^{2-}$  ions diffuse through the Ppy film provoking a decrease of its electrical resistance and an increase of its dielectric constant. From the Warburg impedance coefficient, the sulfate coefficient of diffusion in the Ppy film was  $1.38 \times 10^{-9} \text{ cm}^2 \text{s}^{-1}$ .

**Acknowledgment.** T.J.L.S. is grateful to CONACYT for the stipend received for her Ph.D. studies. The authors are also grateful to CONACYT and PROMEP for the financial support

given through projects 80058 and 46481, respectively. M.P.P. thanks CONACyT for the support through projects 48854 and 24658 ("Nucleación y crecimiento electroquímico de nuevas fases"). M.P.P. and M.R.R. wish to thank the Departamento de Materiales, UAM-A, for the financial support given through projects 2261203, 2261204, and 2261205. J.U. and H.H.H. acknowledge Conacyt for the grant provided to pursue a research sabbatical leave and a postdoctoral position, respectively, in the Departamento de Materiales, UAM-A.

## References and Notes

- (1) Budevski, E.; Staikov, G.; Lorenz, W. J. *Electrochemical Phase Formation. An Introduction to the Initial Stages of Metal Deposition*; VCH: Weinheim, Germany, 1996.
- (2) Milchev, A. *Russ. J. Electrochim.* **2008**, *44*, 619.
- (3) Otero, T. F.; Ariza, M. J. *J. Phys. Chem. B* **2003**, *107*, 13954.
- (4) Garfias-García, E.; Romero-Romo, M.; Ramírez-Silva, M. T.; Morales, J.; Palomar-Pardavé, M. *J. Electroanal. Chem.* **2008**, *613*, 67.
- (5) Branco, D.; Mostany, J.; Borrás, C.; Scharifker, B. R. *J. Solid State Electrochim.* **2009**, *13*, 565.
- (6) Scharifker, B. R.; Mostany, J. In *Encyclopedia of electrochemistry*; Bard, A. J., Stratmann, M., Calvo, E. J., Eds.; Wiley: New York, 2003.
- (7) Fleischmann, M.; Thirsk, H. R. *Trans. Faraday Soc.* **1955**, *51*, 71.
- (8) Gunawardena, G. A.; Hills, G.; Montenegro, I.; Scharifker, B. R. *J. Electroanal. Chem.* **1982**, *138*, 225.
- (9) Palomar-Pardavé, M.; Scharifker, B. R.; Arce, E. M.; Romero-Romo, M. *Electrochim. Acta* **2005**, *50*, 4736.
- (10) Espinoza-Ramos, L. I.; Ramírez, C.; Hallen-López, J. M.; Arce, E.; Palomar-Pardavé, M.; Romero-Romo, M. *J. Electrochim. Soc.* **2002**, *149*, 543.
- (11) Sánchez-Rivera, E.; Vitla-Vaquier, V.; Romero-Romo, M.; Palomar-Pardavé, M.; Ramírez-Silva, M. T. *J. Electrochim. Soc.* **2004**, *151*, 666.
- (12) Álvarez-Romero, G. A.; Garfias-García, E.; Ramírez-Silva, M. T.; Galán Vidal, C.; Romero-Romo, M.; Palomar-Pardavé, M. *Appl. Surf. Sci.* **2006**, *252*, 5783.
- (13) Cobos-Murcia, J. A.; Galicia, L.; Rojas-Hernández, A.; Ramírez-Silva, M. T.; Álvarez-Bustamante, R.; Romero-Romo, M.; Rosquete-Pina, G.; Palomar-Pardavé, M. *Polymer* **2005**, *46*, 9053.
- (14) Loganathan, K.; Pickup, P. G. *Langmuir* **2006**, *22*, 10612.
- (15) Fermín, D. J.; Scharifker, B. R. *J. Electroanal. Chem.* **1993**, *357*, 273.
- (16) Otero, T. F.; Boyano, I. *J. Phys. Chem. B* **2003**, *107*, 6730.
- (17) Heerman, L.; Matthijs, E.; Langerock, S. *Electrochim. Acta* **2001**, *47*, 905.
- (18) Erdy-Gruz, T.; Volmer, M. *Phys. Chem.* **1931**, *165*, 258.
- (19) Bockris, J.; ReddyA. K. N., *Electroquímica Moderna*, 2nd ed.; Reverte: Barcelona, Spain, 1980.
- (20) Greef, R.; Peat, L.; Peter, M.; Pletcher, D.; Robinson, J. *Instrumental Methods in Electrochemistry*; Ellis Horwood: Chichester, UK, 1985; Chapter 9.
- (21) Matthijs, E.; Langerock, S.; Michailova, E.; Heerman, L. *J. Electroanal. Chem.* **2004**, *570*, 123.
- (22) Mendoza-Huizar, L. H.; Robles, J.; Palomar-Pardavé, M. *J. Electroanal. Chem.* **2003**, *545*, 39.
- (23) Zinsmeister, G. *Vacuum* **1966**, *16*, 529.
- (24) Erdy Gruz, T.; Volmer, M. *J. Phys. Chem.* **1931**, *165*, 157.
- (25) Harrison, J. A.; Rangarajan, S. K. *Faraday Symp. Chem. Soc.* **1977**, *12*, 101.
- (26) Bewick, A.; Fleischmann, M.; Thirsk, H. R. *Trans. Faraday Soc.* **1962**, *58*, 2200.
- (27) Armstrong, R. D.; Fleischmann, M.; Thirsk, H. R. *J. Electroanal. Chem.* **1966**, *11*, 208.
- (28) Iroh, J. O.; Zhu, Y.; Shah, K.; Levine, K.; Rajagopalan, R.; Uyar, T.; Donley, M.; Mantz, R.; Johnson, J.; Voevodin, N. N.; Balbyshev, V. N.; Khramov, A. N. *Prog. Org. Coat.* **2003**, *47*, 365.
- (29) Rajagopalan, R.; Iroh, J. O. *Electrochim. Acta* **2002**, *47*, 1847.
- (30) Wencheng, S.; Iroh, J. O. *Electrochim. Acta* **2000**, *46*, 1.
- (31) Skotheim, T. A.; Elsenbaumer, R. L.; Reynolds, J. R., Eds. *Handbook of Conducting Polymers*; Marcel Dekker: New York, 1998.
- (32) Sung, J.; Kim, S.; Lee, K. *J. Power Sources* **2003**, *124*, 343.
- (33) Arrieta, A. A.; Rodríguez, M. L.; Parra, V.; Vegas, A.; Villanueva, S.; Gutiérrez, R.; Saja, J. A. *J. Sens.* **2004**, *4*, 348.
- (34) Li, X.; Zhang, X.; Sun, Q.; Lu, W.; Li, H. *J. Electroanal. Chem.* **2000**, *492*, 23.
- (35) Hwang, B. J.; Santhanam, R.; Wu, C. R.; Tsai, Y. W. *Electroanalysis* **2001**, *13*, 37.
- (36) Colin, C.; Petit, M. A. *J. Electrochim. Soc.* **2002**, *149*, E394.
- (37) Álvarez-Romero, G. A.; Palomar-Pardavé, M. E.; Ramírez-Silva, M. T. *Anal. Bioanal. Chem.* **2007**, *387*, 1533.
- (38) Álvarez-Romero, G.; Morales-Pérez, A.; Rojas-Hernández, A.; Palomar-Pardavé, M.; Ramírez-Silva, M. T. *Electroanalysis* **2004**, *16*, 1236.
- (39) Skotheim, T. A., Ed. *Handbook of Conducting Polymers*; Marcel Dekker: New York, 1986.
- (40) Bobacka, J.; Ivaska, A.; Lewenstam, A. *Electroanalysis* **2003**, *15*, 366.
- (41) Michalska, A.; Nadrycka, U.; Maksymiuk, K. *Anal. Chem.* **2001**, *371*, 35.
- (42) Holzhauser, P.; Bouzek, K. *J. Appl. Electrochim.* **2006**, *36*, 703.
- (43) Weidlich, C.; Mangold, K. M.; Juttner, K. *Electrochim. Acta* **2001**, *47*, 741.
- (44) Wang, J. *Analytical Electrochemistry*, 2nd ed.; Wiley-VCH: New York, 2000.
- (45) Ozylmaz, A. T.; Ozylmaz, G.; Yigitoglu, O. *Prog. Org. Coat.* **2010**, *67*, 28.
- (46) Arenas, M. A.; González Bajos, L.; De Damborenea, J. J.; Ocón, P. *Prog. Org. Coat.* **2008**, *62*, 79.
- (47) Tüken, T.; Tansuó, G.; Yazıcı, B.; Erbil, M. *Prog. Org. Coat.* **2007**, *59*, 88.
- (48) Tüken, T.; Yazıcı, B.; Erbil, M. *Prog. Org. Coat.* **2004**, *51*, 152.
- (49) Licona-Sánchez, T. de J.; Álvarez-Romero, G. A.; Palomar-Pardavé, M. E.; Galán-Vidal, C. A.; Pérez-Hernández, M. E. *ECS Transactions* **2009**, *20*, 31.
- (50) Tietje-Girault, J.; Ponce de León, C.; Walsh, F. C. *Surf. Coat. Technol.* **2007**, *201*, 6025.
- (51) Álvarez-Bustamante, R.; Negrón-Silva, G.; Abreu-Quijano, M.; Herrera-Hernández, H.; Romero-Romo, M.; Cuán, A.; Palomar-Pardavé, M. *Electrochim. Acta* **2009**, *54*, 5393.
- (52) Hsu, C. S.; Mansfeld, F. *Corrosion* **2001**, *57*, 747.
- (53) Vedalakshmi, R.; Saraswathy, V.; Song, H.-W.; Palaniswamy, N. *Corros. Sci.* **2009**, *51*, 1299.
- (54) Suárez, I. J.; Otero, T. F.; Márquez, M. *J. Phys. Chem. B* **2005**, *109*, 1723.
- (55) Otero, T. F.; Márquez, M.; Suárez, I. J. *J. Phys. Chem. B* **2004**, *108*, 15429.
- (56) Kepas, A.; Grzeszczuk, M. *Electrochim. Acta* **2006**, *51*, 4167.

JP102676Q